Controlling Synchronization in Large Laser Networks

Micha Nixon,[1] Moti Fridman,[1] Eitan Ronen,[1] Asher A. Friesem,[1] Nir Davidson,[1] and Ido Kanter[2]
[1]Department of Physics of Complex Systems, Weizmann Institute of Science, Rehovot 76100, Israel
[2]Department of Physics, Bar-Ilan University, Ramat-Gan 52900, Israel
(Received 23 December 2011; published 23 May 2012)

Synchronization in large laser networks with both homogeneous and heterogeneous coupling delay times is examined. The number of synchronized clusters of lasers is established to equal the greatest common divisor of network loops. We experimentally demonstrate up to 16 multicluster phase synchronization scenarios within unidirectional coupled laser networks, whereby synchronization in heterogeneous networks is deduced by mapping to an equivalent homogeneous network. The synchronization in large laser networks is controlled by means of tunable coupling and self-coupling.

DOI: 10.1103/PhysRevLett.108.214101 PACS numbers: 05.45.Xt, 42.25.Kb, 42.55.Rz, 42.60.By

Synchronization in networks with delayed coupling is ubiquitous in nature and plays a key role in almost all fields of science, including physics, biology, ecology, climatology, and sociology [1–7]. In general, the published works on network synchronization are based on data analysis and simulations, with little experimental verification [8–10]. Theoretical investigations suggest that the underlying properties that govern network dynamics can be attributed to either the statistical properties, such as the average number of connections between nodes [11,12], or the detailed distribution of the network connectivity [13,14]. Experimental investigations showed that the symmetry of small networks is related to their synchronization state [7–9]. Recent experimental investigations on small laser networks with homogeneous delay times showed that up to two synchronized clusters can emerge [10]. The number of clusters was limited to two as a result of the bidirectional coupling of light between the lasers. Such a coupling arises from bidirectional propagation of light along the paths that couple the lasers, which is a direct consequence of the time reversal symmetry of light.

Here we develop an approach for multicluster synchronization of larger networks of lasers with homogeneous as well as heterogeneous coupling delay times. In this approach the coupling between lasers is unidirectional, whereby the light propagates only in a single direction along the paths that couple light between the lasers. Such unidirectional coupling is achieved by exploiting the Faraday effect to control the polarization of the lasers' light in order to break the time reversal symmetry of light, and it is essential for obtaining the multicluster synchronization as demonstrated here with up to 16 clusters. We first establish the relationship between the number of the synchronized clusters and the greatest common divisor (GCD) of the number of lasers in different unidirectional network loops. Then, we determine the phase dynamics of heterogeneous networks with commensurate time delays by exploiting a transformation to an equivalent homogenous network that obeys the GCD rules. We also demonstrate how a single connectivity adjustment can affect synchronization throughout the network.

The experimental arrangements are presented in Fig. 1. These include a degenerate laser cavity, a coupling arrangement for controlling the connectivities and obtaining unidirectional couplings between lasers, as well as delayed self-feedback, and a detection arrangement for detecting the far-field (FF) intensity interference pattern from the lasers. The degenerate cavity is comprised of a 10-mm wide Nd:YAG crystal gain medium that can support many independent laser channels [10,15], front and rear output couplers (OC), a mask of an array of apertures of 0.2 mm diameters and 0.3 mm spacing that forms the different laser channels, and two lenses in a $4f$ telescope arrangement. The telescope images the mask plane to the

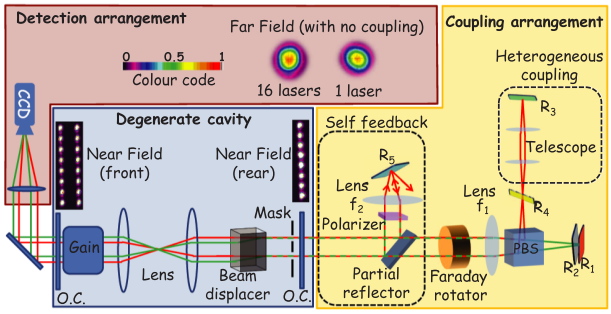

FIG. 1 (color online). A schematic sketch of the experimental arrangements include a degenerate laser cavity, a coupling arrangement and a detection arrangement for detecting the phase synchronization between any desired set of lasers with a CCD camera. The degenerate laser cavity, that supports many independent uncoupled lasers, includes a calcite crystal that displaces each beam into two parallel beams of orthogonal polarization so that a mask with eight apertures leads to 16 lasers, as shown in the insets. The coupling arrangement, with its four coupling mirrors R_1, R_2, R_3, and R_4 that control a variety of different unidirectional homogeneous and heterogenous coupling connectivities, also includes delayed self-feedback coupling controlled by mirror R_5.

front OC plane, thereby eliminating the diffraction of light from one laser to another; this ensures that different lasers do not interact and thus remain uncoupled [10]. Phase independence among the uncoupled lasers is experimentally verified by comparing the FF intensity distributions of a single laser and 16 lasers, shown in the top insets. The lack of interference fringes and the essentially identical distributions indicate that there is no phase synchronization among the 16 lasers. A calcite crystal placed inside the cavity displaces each beam to form two parallel beams with ordinary $\hat{O}$ and extraordinary $\hat{E}$ polarization states, so that a mask with N apertures would lead to $2N$ lasers. From the front of the cavity these $2N$ beams emerge spatially separated, while from the rear they emerge folded onto each other, as shown in the insets for a mask of eight apertures corresponding to 16 independent lasers.

Coupling between lasers is achieved by injecting a delayed light from one laser into another. This is accomplished by means of a focusing lens placed at the focal distance f_1 away from the rear OC of the lasers, a polarizing beam splitter (PBS), and four mirrors that couple light between the lasers. Three coupling mirrors (R_1, R_2 and R_4) are placed within the Rayleigh focal range of the focusing lens and one mirror (R_3) at the image of the focal plane. The imaging is done with a telescope between mirrors R_3 and R_4 so as to further delay the light coupled by R_3. For networks with homogeneous delay time, we resorted to a simpler configuration where R_3 is adjacent to R_4.

With a reflectivity of 40% for R_2 and R_4, and 100% for R_1 and R_3, four nearly equally intense mirror images of the mask plane $E(x, y)$ are reflected back to the lasers to obtain a nearly uniform coupling strength (only a 10% deviation). The Faraday rotator, positioned along the paths of the beams, rotates the polarization state so as to couple $\hat{O}$ polarized lasers to $\hat{E}$ polarized lasers via mirrors R_1 or R_2 and $\hat{E}$ polarized lasers to the $\hat{O}$ polarized lasers via mirrors R_3 or R_4, thereby allowing for unidirectional coupling to occur. Each mirror image $E(-(x - x_0), -(y - y_0))$ can be reflected around a different center point (x_0, y_0) that denotes a self-reflecting point whose location is determined by the angular orientation of the mirror. By independently controlling the angular orientations of all four coupling mirrors, we realized a variety of connectivities between the lasers, whereby each mirror connects pairs of lasers of orthogonal polarizations that are symmetric around its self-reflecting point.

Delayed self-feedback is obtained by using a partial reflector that directs part of the light towards a fifth self-feedback coupling mirror R_5 placed at the focal plane of a focusing lens f_2. This light does not pass through the Faraday rotator so its polarization state is maintained and can be coupled back as delayed self-feedback. By adding the polarizer, we can ensure that only a single laser is self-coupled [16].

Phase synchronization between the lasers is determined by their relative coherence and it is quantified by measuring the fringe visibility of their combined FF intensity interference pattern [17]. In our experiments, the FF intensity interference pattern was detected with a CCD camera that was positioned at the focal plane of a focusing lens, as shown in Fig. 1. A linear polarizer oriented at an angle of 45° (not shown in Fig. 1) was placed before the CCD in order to measure the interference of orthogonally polarized lasers.

In general, the synchronization state of a network is deduced by measuring the interference pattern between all pairs of lasers in the network. In some cases, however, a single measurement of the interference pattern between all lasers together is sufficient to determine the synchronization state. For example, a FF intensity pattern with fringes only along the vertical direction, indicates that synchronization occurs only between lasers positioned along the same vertical column of the laser array. Alternatively, fringes along both the horizontal and vertical directions indicate that synchronization occurs between the lasers that are positioned along both columns and rows of the lasers array.

One specific coupling connectivity is illustrated for a directed loop of 16 lasers in Fig. 2(a), that was obtained by using three coupling mirrors R_1, R_2, and R_4 (red, blue, and green online). The colored arrows in the NF intensity pattern denote which one of the three mirrors led to a specific unidirectional coupling [16]. We found that a directed loop of 16 coupled lasers does not lead to synchronization between any pair of lasers, as verified by the very poor fringe contrast in the FF intensity pattern of all 16 lasers, as shown in Fig. 2(b), left. This is because each laser is synchronized to a signal from its preceding laser along the directed loop that is delayed by τ. With a focusing lens of $f = 30$ cm, the coupling delay time, given by

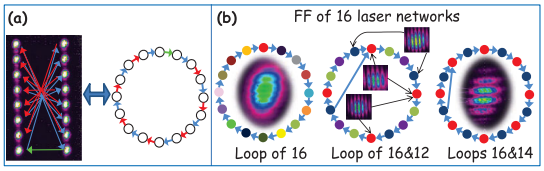

FIG. 2 (color online). (a) Connectivity arrangement in a unidirectional loop of 16 lasers. The colored arrows, added to the near-field intensity distributions of 16 lasers, denote which pairs of lasers are coupled by which mirrors (see mirror colors of Fig. 1 online). (b) Three different networks of 16 lasers, all with 4 ns unidirectional time-delayed couplings. For a single directed loop of 16 lasers, the far-field intensity distribution indicates the lack of synchronization among all 16 lasers (left). For a network with 16 and 12 laser loops, the FF intensity distributions of different pairs of lasers indicates four synchronized clusters, each including lasers marked by a specific color (center). For a network with 16 and 14 laser loops, the FF intensity distribution indicates two separate synchronized clusters (right).

the round trip propagation time through the coupling arrangement is $\tau = 4f/c \approx 4$ ns. Such a delay time is much longer than the coherence time of the lasers $\tau_{coh} \approx 10$ ps, so no isochronal (simultaneous) phase synchronization between the lasers is expected. However, by using the fourth coupling mirror (yellow) to add a unidirectional coupling that forms a new directed loop of 14 lasers, clusters of alternating lasers that are synchronized emerge, as shown in Fig. 2(b), right. The resulting FF intensity pattern with fringes only along the vertical direction indicates that synchronization now occurs only between lasers in the same vertical column. Specifically, the network splits into two distinct synchronized clusters of lasers (denoted by either blue or red colors), i.e., all odd or all even lasers are synchronized, but pairs of odd-even lasers are not synchronized. Alternatively, the fourth coupling mirror could be used to couple between other pairs of lasers so as to form an additional loop of 12 lasers rather than 14 lasers as shown in Fig. 2(b), center. Now, four distinct synchronized clusters emerge, as exemplified by the high contrast interference fringes between pairs of lasers belonging to the same cluster.

The number of synchronized clusters can be predicted in accordance to the network connectivity. Specifically, for homogeneous networks, the number of synchronized clusters is predicted to be equal to the greatest common divisor of the network loops [18–20]. This is consistent with our experimental results [Fig. 2(b)], where a network with 16 and 14 laser loops results in GCD(16, 14) = 2 synchronized clusters, a network of 16 and 12 laser loops results in GCD(16, 12) = 4 synchronized clusters, and a single directed loop of 16 lasers results in GCD(16) = 16 synchronized clusters each comprised of a single laser.

The GCD rule for the number of clusters can be intuitively understood by the fact that each laser synchronizes to the delayed incoming signal and relays the optical phase information onwards in accordance to the network connectivity. As a result, in a directed loop of n lasers with a coupling delay time of τ, each laser is synchronized to its own signal delayed by $n\tau$. Consequently, the signal from each laser has $n\tau$ periodicity, but no synchronized pairs of lasers exists, resulting in n clusters. For a network with an additional loop of m lasers, the signals from all lasers have to fulfil $n\tau$ and $m\tau$ periodicities, resulting in GCD$(n, m)\tau$ periodicity and GCD(n, m) synchronized clusters. Note that other periodic solutions that consist of fewer numbers of clusters also exist but are unstable due to the information mixing mechanism [18,19].

A full quantitative experimental analysis of the multicluster synchronization controlled by the GCD of homogeneous time-delayed networks is exemplified for various eight-laser networks in Fig. 3. A directed loop of eight lasers exhibits no synchronization, whereby there are no interference fringes in the FF intensity pattern in Fig. 3(a). A clear manifestation of the synchronization

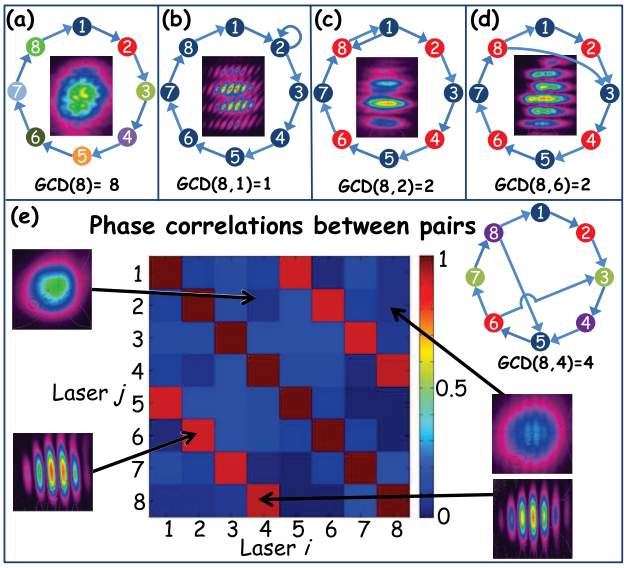

FIG. 3 (color online). (a) A directed loop of eight lasers, where the lack of interference fringes in the FF intensity distribution of all eight lasers indicates no synchronization and eight separate clusters. (b) A directed loop of eight lasers with an additional self-feedback loop, where high contrast interference fringes along both horizontal and vertical directions indicate high synchronization with one cluster GDC(8, 1) = 1. (c) A directed loop of eight lasers with an additional bidirectional loop of size 2, where high contrast interference fringes along the vertical direction only indicate two clusters, GDC(8, 2) = 2. (d) A directed loop of eight lasers with an additional loop of six lasers obtained with unidirectional coupling between laser 8 and laser 3, where high contrast interference fringes along the vertical direction only indicate two clusters, GDC(8, 6) = 2. (e) Phase correlation (fringe visibility) between all pairs of lasers for a network with directed loops of eight and four lasers, indicating four clusters GCD(8, 4) = 4.

state dependence on the detailed network connectivity is exemplified in Fig. 3(b) where a single network connectivity adjustment remotely affects the synchronization state among all lasers. Specifically, the addition of a single self-feedback loop is sufficient to obtain a high degree of global synchronization among all lasers, forming a single synchronized cluster GCD(8, 1) = 1. The high contrast interference fringes, with a visibility above 0.9, appearing along both vertical and horizontal directions in the FF intensity pattern in Fig. 3(b), indicate that synchronization indeed occurs among all lasers in the network. When a single bidirectional coupling channel is added to the directed loop, a loop of two lasers is formed resulting in GCD(8, 2) = 2 synchronized clusters. The high contrast interference fringes, with a visibility of 0.88, appearing along the vertical axis only in the FF intensity pattern in Fig. 3(c), indicate that synchronization occurs only between lasers in the same vertical column. Alternatively, two clusters can also be formed by adding unidirectional coupling from laser 8 to laser 3 to obtain a six-laser loop

and GCD(8, 6) = 2 clusters. Here again, the high contrast interference fringes in Fig. 3(d), with a visibility of 0.89, appearing only along the vertical axis indicate two synchronized clusters.

A network consisting of four and eight laser loops results in GCD(8, 4) = 4 clusters. The synchronization state for such a network was quantified by measuring the fringe visibility between all possible 28 pairs of lasers, as presented in Fig. 3(e). Representative FF interference patterns for pairs of lasers that were used to calculate the fringe visibility are shown in the insets. The fringe visibility was above 0.9 for all pairs of lasers that belong to the same cluster and below 0.15 otherwise. These results clearly indicate the existence of four distinct synchronized clusters.

The established GCD rule only applies to homogeneous networks. Thus, we extend the GCD rule to include the dynamics of heterogeneous networks with commensurate ratios among the delays [21]. This extension is achieved by resorting to equivalent homogeneous networks where imaginary lasers are added so as to split delays to homogeneously shorter delay segments. Then, we apply the GCD rule to the equivalent homogeneous network to find the actual number of clusters in the heterogeneous network. We experimentally examined a heterogeneous network of six lasers with τ and 2τ time delays, as shown in Fig. 4(a), upper sketch. The equivalent homogenous network consists of two additional imaginary lasers so as to form eight and six laser loops as shown in Fig. 4(a), lower sketch, leading to two synchronized clusters GCD(8, 6) = 2. The experimental results indeed revealed two synchronized clusters, lasers 1, 4, and 5, and lasers 2, 3, and 6. The visibility of the interference fringes in the FF patterns in Fig. 4(a) was above 0.8 for any pair of lasers that belong to the same cluster and below 0.1 otherwise. The role of the GCD was further examined for a more compound heterogeneous network consisting of eight lasers and three different time delays, τ, $\tau/2$, and $3\tau/2$, as shown in Fig. 4(b), upper sketch. The equivalent homogenous network with equal time delays of $\tau/2$ has an additional nine imaginary lasers that form a directed loop of 17 lasers with an additional single self-feedback loop, as shown in Fig. 4(b), lower sketch. This equivalent homogeneous network has one synchronized cluster GCD(17, 1) = 1, as confirmed by the high contrast fringes in the FF interference pattern in Fig. 4(b) of all the eight lasers.

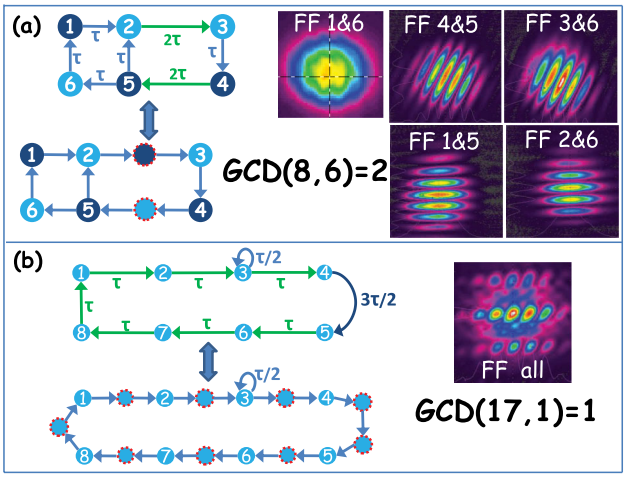

FIG. 4 (color online). (a) Heterogeneous network of six lasers with $\tau = 4$ ns and $2\tau = 8$ ns time delays (top) and the equivalent homogenous network of eight lasers (bottom). The FF interference patterns of different pairs of lasers indicate the formation of two clusters GCD(8, 6) = 2. (b) Heterogeneous network of eight lasers with $\tau = 4$ ns, $\tau/2 = 2$ ns, and $3\tau/2 = 6$ ns time delays (top) and the equivalent homogenous network of 17 lasers (bottom). The FF interference pattern of all lasers indicates a single synchronized cluster GCD(17, 1) = 1.

It should be noted that the mapping of heterogeneous networks to homogeneous networks by the addition of imaginary lasers is valid only when they act as transparent devices that relay the signal they receive to the next laser along the coupling path. Our experimental results indicate that such a mapping is sufficiently accurate for phase synchronization. However, simulation of intensity synchronization of chaotic diode lasers suggest that in some cases, the additional lasers may not act as simple transparent devices but relay a different chaotic signal onward [18]. Consequently, further investigations are required to ascertain the validity of the mapping of heterogeneous networks to homogeneous networks for intensity synchronization of chaotic diode lasers.

To conclude, we demonstrated multicluster synchronization of large networks of unidirectional coupled lasers with homogeneous as well as heterogeneous delay times, and investigated the effects of self-feedback coupling. It should be noted that although we observed a high level of synchronization with fringe visibility values (0.8) for networks of 8 and 16 lasers, we expect that level of synchronization would eventually degrade as the network size increases [23]. However, further investigations are required to ascertain the exact nature of finite size effects in time-delayed coupled networks.

We numerically confirmed the role of GCD for phase synchronization of homogeneous and heterogeneous delay networks using the Kuramoto model that describes a general class of oscillators [16]. Accordingly, our approach and results could be applied to a variety of coupled oscillators in electrical, biological, chemical, and climatic phenomena.

The work was supported in part by the United States-Israel Binational Science Foundation and the ISF Bikura grant.

[1] S. H. Strogatz, Nature (London) **410**, 268 (2001).
[2] E. Schoell, Nature Phys. **6**, 161 (2010).
[3] H. G. Schuster and W. Just, *Deterministic Chaos* (Wiley-VCH, Weinheim, 2005).

[4] R. Albert and A.-L. Barabasi, Rev. Mod. Phys. **74**, 47 (2002).
[5] M. E. J. Newman, SIAM Rev. **45**, 167 (2003).
[6] K. E. Callan, L. Illing, Z. Gao, D. J. Gauthier, and E. Scholl, Phys. Rev. Lett. **104**, 113901 (2010).
[7] A. Takamatsu, R. Tanaka, H. Yamada, T. Nakagaki, T. Fujii, and I. Endo, Phys. Rev. Lett. **87**, 7 (2001).
[8] J. R. Terry, K. S. Thornburg Jr., D. J. DeShazer, G. D. VanWiggeren, S. Zhu, P. Ashwin, and R. Roy, Phys. Rev. E **59**, 4036 (1999).
[9] B. Ravoori, A. B. Cohen, J. Sun, A. E. Motter, T. E. Murphy, and R. Roy, Phys. Rev. Lett. **107**, 034102 (2011).
[10] M. Nixon, M. Fridman, E. Ronen, A. A. Friesem, N. Davidson, and I. Kanter, Phys. Rev. Lett. **106**, 223901 (2011).
[11] A.-L. Barabasi and R. Albert, Science **286**, 509 (1999).
[12] C. Masoller and A. C. Marti, Phys. Rev. Lett. **94**, 134102 (2005).
[13] V. Flunkert, S. Yanchuk, T. Dahms, and E. Scholl, Phys. Rev. Lett. **105**, 254101 (2010).
[14] J. Jost and M. P. Joy, Phys. Rev. E **65**, 016201 (2001).
[15] J. A. Arnaud, Appl. Opt. **8**, 1909 (1969).
[16] See Supplemental Material at http://link.aps.org/supplemental/10.1103/PhysRevLett.108.214101 for more information regarding the coupling and self-feedback experimental arrangements, remote switching to control the number of clusters, and numerical result.
[17] R. Loudon, *The Quantum Theory of Light* (Oxford, New York, 2001), 3rd ed..
[18] I. Kanter, E. Kopelowitz, R. Vardi, M. Zigzag, W. Kinzel, M. Abeles, and D. Cohen, Europhys. Lett. **93**, 66001 (2011).
[19] I. Kanter, M. Zigzag, A. Englert, F. Geissler, and W. Kinzel, Europhys. Lett. **93**, 60003 (2011).
[20] T. W. Wu, W. Z. Chang, A. Galvanauskas, and H. G. Winful, Opt. Express **18**, 25873 (2010).
[21] Commensurate ratios are defined within the resolution of the coherence time [22].
[22] M. Nixon, M. Fridman, E. Ronen, A. A. Friesem, and N. Davidson, Opt. Lett. **34**, 1864 (2009).
[23] F. Rogister, K. S. Thornburg, L. Fabiny, M. Moller, and R. Roy, Phys. Rev. Lett. **92**, 093905 (2004).